Proceedings Paper:
Wang, Y., Davidson, J.N. and Foster, M.P. (2022) Cyclic-mode modelling of class EF2 inverters featuring a piezoelectric resonator as the auxiliary network. In: 11th International Conference on Power Electronics, Machines and Drives (PEMD 2022). PEMD 2022 - The 11th International Conference on Power Electronics, Machines and Drives, 21-23 Jun 2022, Newcastle, UK (hybrid conference). IET Digital Library, pp. 131-135. ISBN: 9781839537189.

https://doi.org/10.1049/icp.2022.1120

Cyclic-mode modelling of class EF_2 inverters featuring a piezoelectric resonator as the auxiliary network

Yuqing Wang, Jonathan N. Davidson, Martin P. Foster

Department of Electronic and Electrical Engineering, University of Sheffield, Sheffield, UK.
Email: ywang359@sheffield.ac.uk

Keywords: Resonant inverter, Class EF inverter, Piezo resonator, Cyclic model.

Abstract

By connecting an auxiliary network in parallel with the switch in a class E inverter, class EF resonant inverters are able to reduce the voltage stresses on the switch. This paper presents a cyclic mode model for predicting the behaviour class EF inverters that use a piezoelectric resonator in place of the resonant circuit. The performance of the proposed model is validated using a Class EF_2 resonant inverter where the piezoelectric resonator is tuned to twice the main branch resonant frequency.

1 Introduction

Single-switch power supply circuits are popular due to their low component count and consequently low cost. The flyback converter is the most well-known single switch converter but as switching frequencies increase in the pursuit of smaller power supplies, switching losses and the effects of parasitic components become problematic. Class E resonant inverters emerged to solve these problems by employing resonance to achieve zero voltage switching (ZVS) [1]. Class E inverters have been reported to achieve high efficiency operating in the MHz range. Unfortunately, due to resonance, class E inverters exhibit high switch stresses. During regular operation, the peak switch voltage may exceed 3.5 times the input voltage, which poses voltage rating difficulties for the switching device and the parallel capacitor.

With Class EF inverters, an auxiliary series LC branch is connected in parallel with the switch, and careful design ensures that the resonant frequency of the auxiliary LC circuit is specifically tuned to reduce the peak switch voltage. In [2] Aldhaher, *et al*., found that the class EF_2 inverter, where the resonant frequency of the auxiliary branch is tuned to double the inverter operating frequency, has the best performance. The switch voltage of the class EF_2 inverter can be reduced from 3.5 times the power supply voltage by class E inverter to 2.1 times the power supply voltage. However, this improvement is at the expense of volume and complexity.

Piezoelectric resonating devices provide an exciting alternative to discrete component LC resonant networks. Piezoelectric transformers (PTs) have been popular for many years in ionising and cold-cathode fluorescent backlighting applications [3]. Compared with magnetic materials, PTs have notable advantages. The first is that their power density is relatively large at around 40 W/cm^3 [4]. Therefore, under the conditions of transmitting the same power, PTs usually have a smaller volume. They also do not require copper windings, significantly reducing the copper used in the manufacturing process. They can also provide a higher voltage transformation ratio than a magnetic transformer. Recently DC-DC power supply circuits have emerged that utilise a piezoelectric resonator (akin to a one-port PT) as a resonant circuit to efficiently transfer energy [5]. In [6], a class EF_2 inverter utilising a piezoelectric resonator as the auxiliary circuit was described.

Here, a cyclic-mode model for a class EF_2 inverter with a piezoelectric auxiliary circuit is described. The model provides an exact analysis and can be used for design validation and to investigate ZVS performance.

2 Operation of class EF_2 inverter

Fig. 1 shows the circuit of a class EF_2 inverter. L_s and C_s form the main resonant branch, which forces a sinusoidal shaped current to flow through the load R_L. $Q1$ is the MOSFET switch and is operated at a frequency f_{sw}, which close to the L_s C_s resonant frequency of $f_0 = {}^{1}/_{2\pi\sqrt{L_s C_s}}$ and with a duty D. Input inductor L_{in} is a filter inductor ensuring that only a DC current i_{Lin} from the input voltage V_{in}. $X1$ is the piezoelectric resonator with the equivalent circuit shown in Fig.2.

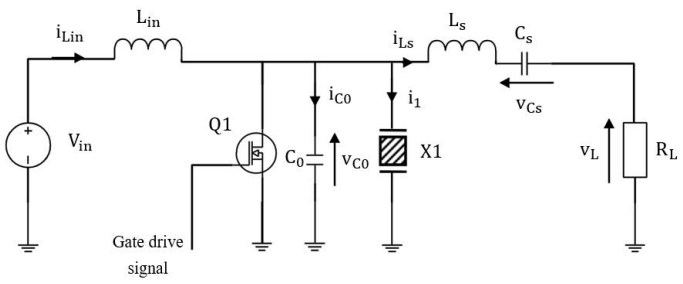

Fig. 1. Circuit diagram of class EF_2 inverter

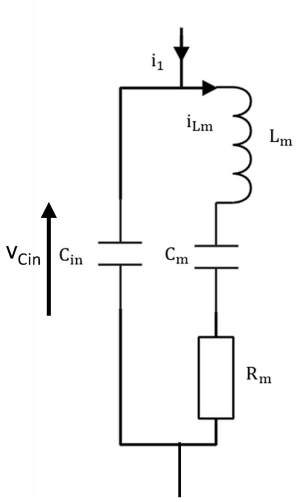

Fig. 2. Circuit diagram of a Piezo-resonator[7]

The following assumptions are usually made when designing class EF_2 inverters:

- L_{in} is large, thus the input current i_{Lin} can be considered to be ripple-free
- the loaded quality factor of the main resonant branch is sufficient to ensure the current through the load is sinusoidal ($Q = \frac{\omega_0 L_s}{R_L} > 5, \omega_0 = 2\pi f_0$)
- the resonant frequency f_0 of the series LC branch should be lower than the operating frequency f_{sw}.

With these conditions, the operation of the inverter can be decomposed into three modes (shown in Fig. 3) during a single switching period. Set $T_{sw} = 1/f_{sw}$.

Mode 1 (M1): $Q1$ turned on for a period D/f_{sw} . During this time, the switch voltage and the resonator voltage is zero. V_{in} is applied to L_{in}.

Mode 2 (M2): $Q1$ is turned off. Current flows out of L_{in} and into C_0, the piezoelectric resonator $X1$ and the main resonant branch. $i_{Lin} = i_{C0} + i_1 + i_{Ls}$. Since the current is flowing into the resonator, its voltage increases from zero to a maximum value and then reduces.

Mode 3 (M3): $Q1$ remains turned off, and the voltage v_{DS} falls below zero, turning on $Q1's$ body diode.

If the choice of f_{sw} and D is appropriate, then the inverter operates with only two modes in the following sequence M1-M2-M1-M2-…, shown in Fig. 3a. Zero voltage switching (ZVS) can be achieved if $v_{DS}(T_{sw}) = 0$. If v_{DS} falls below zero before $t = T_{sw}$ and thereby turning on $Q1$'s body diode then, the circuit enters M3 and sequence then becomes M1-M2-M3-M1…, shown in Fig. 3b. Time t_0 is the start of the cycle and the start of Mode 1, then $t_1 = DT_{sw}$ is the end of Mode1 and the start of Mode 2 with t_2 being the end of Mode 2, which is also the start of Mode 1 for the two-mode operation cycle shown in Fig. 3a. For three modes of operation the MOSFET body diode starts conducting at t_2 and the cycle ends at t_3 when $Q1$ is turned-on again. This paper assumes an appropriate choice of switching frequency and duty has been made to ensure the class EF_2 inverter operates with the two-mode operating sequence M1-M2-M1…

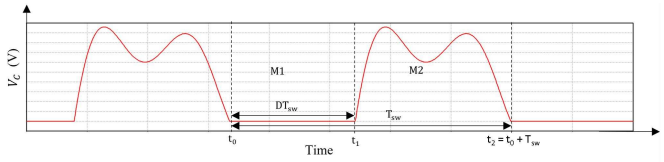

(a)

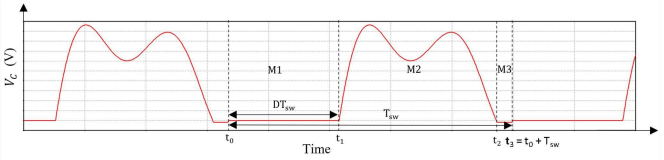

(b)

Fig. 3. Example switch voltage waveform of 2 mode operation (a) and 3 mode operation (b)

Since there are only two piecewise linear state-variable models per cycle, cyclic mode analysis can directly obtain the inverter's initial condition. Subsequently, the state variable value can be determined at any time throughout the cyclic mode [8].

3 Derivation of cyclic-mode model for class EF_2 inverter

To build the inverter's cyclic model, the first-order differential equations are needed to describe the derivatives of the capacitor voltages and the inductor currents. Since C_0 and C_{in} are connected in parallel, they are combined into a single capacitor to simplify the following analysis.

$$C = C_0 + C_{in} \tag{1}$$

For Mode 1 (M1) $t_0 \le t < t_1$:
The switch is turned on, and the derivative of the input inductor current is given by,

$$\dot{i_{Lin}} = \frac{v_{Lin}}{L_{in}} = \frac{V_{in}}{L_{in}} \tag{2}$$

With the derivative being denoted by $\dot{z} \equiv \frac{dz}{dt}$. The series inductor current is found from,

$$\dot{i_{Ls}} = \frac{v_{Lin}}{L_s} = \frac{-v_{Cs} - R_L i_{Ls}}{L_s} \tag{3}$$

The piezoelectric resonator's (PR) equivalent inductor current is found from,

$$\dot{i_{Lm}} = \frac{-v_{Cm} - i_{Lm} R_m}{L_m} \tag{4}$$

Since the switch is turned on, $v_{DS} = v_{C0} = v_{Cin} = v_C = 0$. Thus,

$$\dot{v_C} = 0 \tag{5}$$

For the series capacitor,

$$\dot{v_{Cs}} = \frac{i_{Cs}}{C_s} = \frac{i_{Ls}}{C_s} \tag{6}$$

And for the piezoelectric resonator,

$$\dot{v_{Cm}} = \frac{i_{Cm}}{C_m} = \frac{i_{Lm}}{C_m} \tag{7}$$

Combining (2)-(7) gives the state-variable model for M1,

$$\begin{bmatrix} \dot{i_{Lin}} \\ \dot{i_{Ls}} \\ \dot{i_{Lm}} \\ \dot{v_C} \\ \dot{v_{Cs}} \\ \dot{v_{Cm}} \end{bmatrix} = \begin{bmatrix} 0 & 0 & 0 & 0 & 0 & 0 \\ 0 & -\frac{R_L}{L_s} & 0 & 0 & -\frac{1}{L_s} & 0 \\ 0 & 0 & -\frac{R_m}{L_m} & 0 & 0 & -\frac{1}{L_m} \\ 0 & 0 & 0 & 0 & 0 & 0 \\ 0 & \frac{1}{C_s} & 0 & 0 & 0 & 0 \\ 0 & 0 & \frac{1}{C_m} & 0 & 0 & 0 \end{bmatrix} \begin{bmatrix} i_{Lin} \\ i_{Ls} \\ i_{Lm} \\ v_C \\ v_{Cs} \\ v_{Cm} \end{bmatrix} + \begin{bmatrix} \frac{V_{in}}{L_{in}} \\ 0 \\ 0 \\ 0 \\ 0 \\ 0 \end{bmatrix} \tag{8}$$

Equation (8) can be rewritten as

$$\dot{\boldsymbol{x}} = \boldsymbol{A_1}x + \boldsymbol{B_1} \tag{9}$$

where the state-vector $\boldsymbol{x} = [i_{Lin}\ i_{Ls}\ i_{Lm}\ v_C\ v_{Cs}\ v_{Cm}]^{\mathrm{T}}$

For Mode 2 (M2) $t_1 \le t < t_2$,
The MOSFET is turned off, and so charge can build upon C_0 and C_{in}. The input inductor current is described by,

$$\dot{i_{Lin}} = \frac{V_{in} - v_C}{L_{in}} \tag{10}$$

The series inductor current is found from

$$\dot{i_{Ls}} = \frac{v_C - v_{Cs} - R_L i_{Ls}}{L_s} \tag{11}$$

The PR's equivalent inductor current is found from

$$\dot{i_{Lm}} = \frac{v_C - v_{Cm} - i_{Lm}R_m}{L_m} \tag{12}$$

The equivalent capacitor voltage, which is also equal to the MOSFET drain-source voltage, is given by,

$$\dot{v_C} = \frac{i_{Lin} - i_{Ls} - i_{Lm}}{C} \tag{13}$$

For the series capacitor voltage,

$$\dot{v_{Cs}} = \frac{i_{Ls}}{C_s} \tag{14}$$

The PR's equivalent capacitor voltage,

$$\dot{v_{Cm}} = \frac{i_{Lm}}{C_m} \tag{15}$$

Combining (10)-(15) provides a state-variable model for Mode 2,

$$\begin{bmatrix} \dot{i_{Lin}} \\ \dot{i_{Ls}} \\ \dot{i_{Lm}} \\ \dot{v_C} \\ \dot{v_{Cs}} \\ \dot{v_{Cm}} \end{bmatrix} = \begin{bmatrix} 0 & 0 & 0 & -\frac{1}{L_{in}} & 0 & 0 \\ 0 & -\frac{R_L}{L_s} & 0 & \frac{1}{L_s} & -\frac{1}{L_s} & 0 \\ 0 & 0 & -\frac{R_m}{L_m} & \frac{1}{L_m} & 0 & -\frac{1}{L_m} \\ \frac{1}{C} & -\frac{1}{C} & -\frac{1}{C} & 0 & 0 & 0 \\ 0 & \frac{1}{C_s} & 0 & 0 & 0 & 0 \\ 0 & 0 & \frac{1}{C_m} & 0 & 0 & 0 \end{bmatrix} \begin{bmatrix} i_{Lin} \\ i_{Ls} \\ i_{Lm} \\ v_C \\ v_{Cs} \\ v_{Cm} \end{bmatrix} + \begin{bmatrix} \frac{V_{in}}{L_{in}} \\ 0 \\ 0 \\ 0 \\ 0 \\ 0 \end{bmatrix} = \boldsymbol{A_2}x + \boldsymbol{B_2} \tag{16}$$

Thus, (8) and (16) can be combined in a piecewise linear equation dependent on the mode duration times.

$$\dot{\boldsymbol{x}}(t) = \begin{cases} \boldsymbol{A_1}x + \boldsymbol{B_1} & t_0 \le t < t_1 \\ \boldsymbol{A_2}x + \boldsymbol{B_2} & t_1 \le t < t_2 \end{cases} \tag{17}$$

Since the class EF_2 inverter is operating in a cyclic mode, the final condition of state variables at the end of cycle $\boldsymbol{x}(t_2)$ should equal the initial condition of that cycle $\boldsymbol{x}(t_0)$. Thus,

$$\boldsymbol{x}(t_0) = \boldsymbol{x}(t_2) = \boldsymbol{x}(t_0 + T_{sw}) \tag{18}$$

since $t_2 = T_{sw}$. Starting from $t = t_0$, the state-vector at the end of Mode 1 is given by,

$$\boldsymbol{x}(\boldsymbol{t_1}) = \boldsymbol{\Phi_1}\boldsymbol{x}(\boldsymbol{t_0}) + \boldsymbol{\Gamma_1} \tag{19}$$

where $\boldsymbol{\Phi_1} = e^{\boldsymbol{A_1}(t_1 - t_0)} = e^{\boldsymbol{A_1}DT_{sw}}$ and $\boldsymbol{\Gamma_1} = \boldsymbol{A_1^{-1}}[\boldsymbol{\Phi_1} - \boldsymbol{I}]\boldsymbol{B_1}$
Similarly, the state-vector at the end of Mode 2 is given by,

$$\boldsymbol{x}(\boldsymbol{t_2^-}) = \boldsymbol{\Phi_2}\boldsymbol{x}(\boldsymbol{t_1}) + \boldsymbol{\Gamma_2} \tag{20}$$

where $\boldsymbol{\Phi_2} = e^{\boldsymbol{A_2}(t_2 - t_1)} = e^{\boldsymbol{A_2}(1-D)T_{sw}}$ and $\boldsymbol{\Gamma_2} = \boldsymbol{A_2^{-1}}[\boldsymbol{\Phi_2} - \mathbf{I}]\boldsymbol{B_2}$. It should be noted that a discontinuity may occur at the end of Mode 2 if $v_C \neq 0$ which is accounted for by forcing $v_C(t_2) = 0$,

$$\boldsymbol{x}(t_0) = \boldsymbol{x}(t_2) = \boldsymbol{K}\boldsymbol{x}(t_2^-) \tag{21}$$

where,

$$\boldsymbol{K} = \begin{bmatrix} 1 & 0 & 0 & 0 & 0 & 0 \\ 0 & 1 & 0 & 0 & 0 & 0 \\ 0 & 0 & 1 & 0 & 0 & 0 \\ 0 & 0 & 0 & 0 & 0 & 0 \\ 0 & 0 & 0 & 0 & 1 & 0 \\ 0 & 0 & 0 & 0 & 0 & 1 \end{bmatrix} \tag{22}$$

The cyclic-mode initial condition $x(t_0)$ can be found by evaluating the final conditions of each mode [9]. Substituting (19) into (20) gives,

$$\begin{aligned} \boldsymbol{x}(t_2^-) &= \boldsymbol{\Phi_2}\boldsymbol{x}(t_1) + \boldsymbol{\Gamma_2} \\ &= \boldsymbol{\Phi_2}\boldsymbol{\Phi_1}\boldsymbol{x}(t_0) + \boldsymbol{\Phi_2}\boldsymbol{\Gamma_1} + \boldsymbol{\Gamma_2} \end{aligned} \tag{23}$$

Combining with (23) and (21) to get

$$\boldsymbol{x}(t_0) = \boldsymbol{K}[\boldsymbol{\Phi_2}\boldsymbol{\Phi_1}\boldsymbol{x}(t_0) + \boldsymbol{\Phi_2}\boldsymbol{\Gamma}_1 + \boldsymbol{\Gamma_2}] \tag{24}$$

So,

$$\boldsymbol{x}(t_0) = [\boldsymbol{I} - \boldsymbol{K}\boldsymbol{\Phi_2}\boldsymbol{\Phi_1}]^{-1}\boldsymbol{K}[\boldsymbol{\Phi_2}\boldsymbol{\Gamma_1} + \boldsymbol{\Gamma_2}] \tag{25}$$

With $\boldsymbol{x}(t_0)$ obtained, then $\boldsymbol{x}(t_1)$ is determined from (19).

Finally, the state variable value at every time can be determined by,

$$\boldsymbol{x}(t) = \begin{cases} \boldsymbol{\Phi_1}(t)\boldsymbol{x}(t_0) + \boldsymbol{\Gamma_1}(t) & t_0 \le t < t_1 \\ \boldsymbol{\Phi_2}(t)\boldsymbol{x}(t_1) + \boldsymbol{\Gamma_2}(t) & t_1 \le t < t_2 \end{cases} \quad (26)$$

Where 1 and 2 is the mode index, $\boldsymbol{\Phi_i}(t) = e^{\boldsymbol{A_i}(t-t_{i-1})}$ and $\boldsymbol{\Gamma_i}(t) = \boldsymbol{A_i}^{-1}[\boldsymbol{\Phi}_i(t) - \boldsymbol{I}]\boldsymbol{B}_i$.

3 Model validation

To validate the proposed model, a prototype class EF_2 inverter featuring a PR was developed. The inverter utilises a STEMiNC SMD25T85F234S piezoelectric resonator [10]. The device was characterised using an Omicron Bode 100 vector network analyser. The resonant frequency was measured as f_0 = 86.291 kHz. Based on the PR equivalent circuit, the main branch components were determined using Aldhaher, *et al.*, [3] design methodology. The components values for the design are listed in Table 1.

Table 1 Inverter components value

Component's name	Component's value
R_m	4.27 Ω
L_m	8.25 mH
C_m	0.412 nF
C_{in}	1.04 nF
C_0	20 nF
L_{in}	10 mH
L_s	0.8 mH
C_s	22.5 nF
R_L	40 Ω
V_{in}	15 V

The duty cycle and frequency were set to D = 0.36 and f_{sw} = 43.14 kHz. Fig. 4 shows the comparison of experimental switch voltage with cyclic model switch voltage. The solid line is the experimental result, and the dotted line is the cyclic model result. The maximum cyclic model voltage is 30.7 V, but the maximum experimental switch voltage is 27.9 V.

To demonstrate the advantage of the class EF_2 topology, the circuit is forced to operate as a class E inverter by disconnecting the auxiliary network. Fig.5 shows the switch voltage reaching of the maximum of 44V.

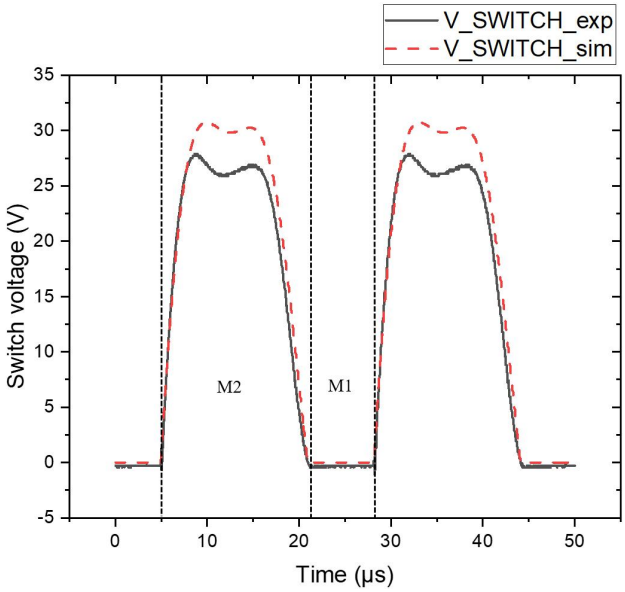

Fig. 4. The switch voltage v_{C0} waveform of cyclic model and experiment circuit

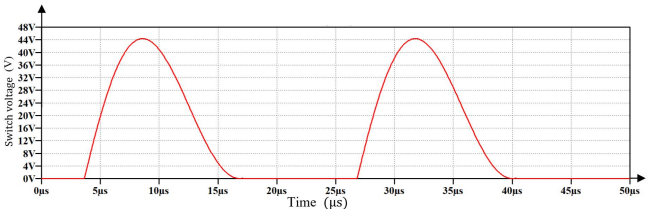

Fig. 5. Switch voltage v_{C0} of class E inverter circuit

Fig.6 is a comparison of simulation with experimental load voltage for the class EF_2 converter. The solid line is the experimental result, and the dotted line is the simulation result. The cyclic model peak-peak load voltage is 17.28 V for an output power of 0.93 W. The experimental peak-o-peak load voltage is 16.78 V. This means the output power is 0.88 W.

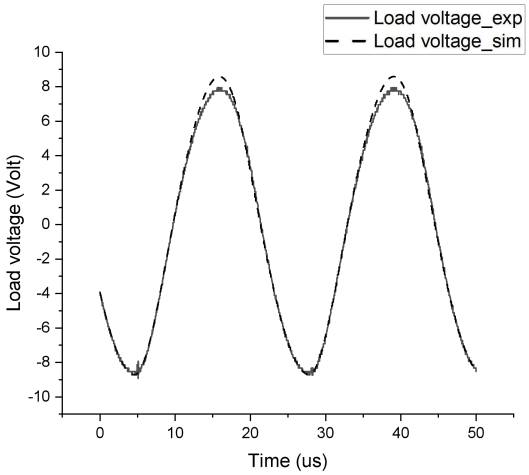

Fig. 6. Load voltage v_L of cyclic model and experiment circuit

In order to prove the function of the piezoelectric resonator, the piezoelectric resonator was replaced with a standard capacitor and inductor. Fig.7 shows experimental

measurements of the switch voltage and load voltage. The maximum switch voltage is 30.4 V, the peak-to-peak load voltage is 16.2 V and the output power is 0.82 W.

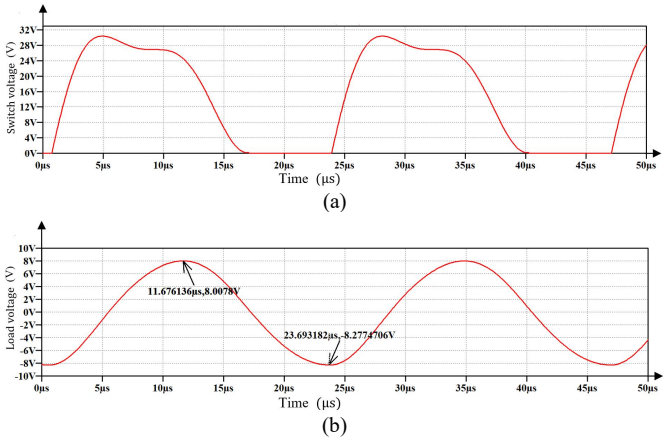

Fig. 7. Class EF_2 inverter's switch voltage (a) and load voltage (b) which uses standard inductor and capacitor as auxiliary network

As for the performance of class EF_2 inverter, Fig.5 shows the maximum voltage of the class E inverter is 46% higher than the class EF_2 inverter. Then according to Fig.4, the maximum experimental voltage is 3 V lower than the cyclic model result. This difference may be due to parasitic impedance of capacitors and inductors that have not been accounted for in the cyclic model. The experimental load voltage is very close to the cyclic model result, with an error of less than 3%. The last figure shows that using a standard inductor and capacitor to replace PR will cause more loss and decrease output power.

4 Conclusion

In summary, the cyclic model shows good accuracy at load voltage prediction. Employing a piezo resonator for the auxiliary circuit can reduce the power loss and increase output power. The future work is to refine the model to improve the accuracy of switch voltage prediction and adjust the circuit board to minimise the effect of parasitic components.

5 References

[1] Kazimierczuk, Marian K. and Dariusz Czarkowski. 'Resonant power converters' (John Wiley & Sons, 2nd edn. 2012)

[2] Aldhaher S, Yates D C and Mitcheson P D. 'Modeling and analysis of class EF and class E/F inverters with series-tuned resonant networks' IEEE Transactions on Power Electronics (TPEL), 2015, 31(5): 3415-3430.

[3] Tien Huang Y, Kung Lee C, Jong Wu W. 'High-powered backlight inverter for LCD-TVs using piezoelectric transformers' Journal of Intelligent Material Systems and Structures (J INTEL MAT SYST STR), 2007, 18(6): 601-609.

[4] Carazo A V. '50 years of piezoelectric transformers. Trends in the technology'. MRS Online Proceedings Library (OPL), 2003, 785.

[5] Touhamit M, Despesse G and Costa F. 'A New Topology of DC-DC Converter Based on Piezoelectric Resonator'. 2020 IEEE 21st Workshop on Control and Modeling for Power Electronics (COMPEL). IEEE, 2020: 1-7.

[6] Vincent M, Ghislain D, Sebastien C. 'A new topology of resonant inverter including a piezoelectric component'. 2021 European Conference on Power Electronices and Applications (ECCE). EPE, 2021.

[7] Forrester J, Davidson J, Foster M, et al. 'Equivalent circuit parameter extraction methods for piezoelectric transformers' 2019 21st European Conference on Power Electronics and Applications (EPE'19 ECCE Europe). IEEE, 2019.

[8] Visser H R, Van den Bosch P J. 'Modelling of periodically switching networks' PESC'91 Record 22nd Annual IEEE Power Electronics Specialists Conference. IEEE, 1991: 67-73.

[9] Foster M P, Horsley E L, Stone D A. 'Predicting the zero-voltage switching profiles of half-bridge driven inductor-less piezoelectric transformer-based inverters' IET Power Electronics, 2012, 5(7): 1068-1073.

[10] 'STEMiNC Steiner & Martins. Piezoelectric disc information'. https://www.steminc.com/PZT/en/piezoelectric-disc25x85mm-s-235-khz. Accessed 28 October 2021